Volume 1 | Number 1 | Jan 2013 | Pages 1–100

PCCP

Physical Chemistry Chemical Physics
www.rsc.org/pccp

ROYAL SOCIETY OF CHEMISTRY
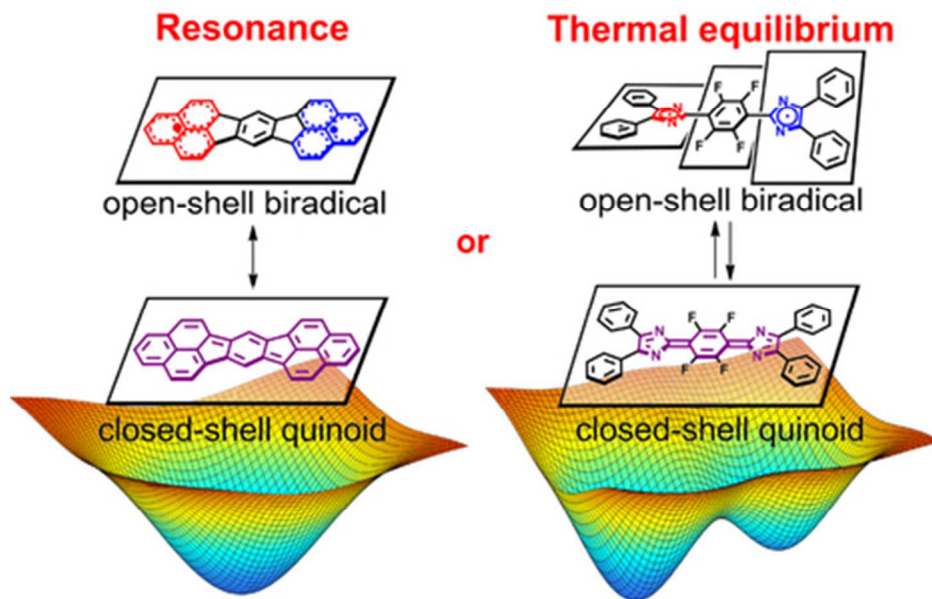
The valence isomerization from the photogenerated biradical to the quinoid species is observed for the photochromic dimer of imidazolyl radicals.
39x25mm (300 x 300 DPI)

PCCP

ARTICLE

Entropy-Controlled Biradical–Quinoid Isomerization of A π-Conjugated Delocalized Biradical

Katsuya Mutoh,[a] Yuki Nakagawa,[b] Sayaka Hatano,[c] Yoichi Kobayashi,[a] and Jiro Abe*[ad]

Biradicaloid species have been extensively studied for their characteristic features in electric conductivity, magnetism, and optical nonlinearity. Theoretical investigations of rigid biradicaloid species have been suggesting that they are represented as a resonance hybrid of open-shell biradical and closed-shell quinoid structures. However, much is still unknown about flexible biradicaloid species whether the activation free energy barrier between these states exists or not. Herein, we investigated the thermal isomerization from the photogenerated unstable biradical to the stable quinoid species observed for the photochromic dimer of a bisimidazolyl radical and found that the large negative activation entropy for the valence isomerization causes the activation free energy barrier between these two states.

Introduction

In recent years, considerable interest has been focused on the chemistry of biradicaloid species[1–5] because of their unique electronic,[6–8] optical[9–15] and magnetic properties.[13,16–19] Open-shell polycyclic aromatic hydrocarbons (PAH) represented by phenalenyl derivatives have been widely studied to make better use of the attractive features of biradicaloid species.[6,13,20–23] PAHs have two representative resonance forms, *i.e.* an open-shell biradical structure and a closed-shell quinoid structure. The geometrical differences between these structures are supposed to be small due to the rigid molecular frameworks (Fig. 1a). However, the resonance hybrid of these structures results in the singlet biradical character in the ground state of PAHs. On the other hand, some reports have given controversial subjects for the electronic structures of biradicaloid species possessing flexible molecular structures such as Chichibabin's hydrocarbon and 1,4-bis-(4,5-diphenylimidazol-2-ylidene)-cyclohexa-2,5-diene (BDPI-2Y) derivatives (Fig. 1b).[24–29] Though the possibility of the thermal equilibrium between the open-shell biradical state and the closed-shell quinoid state of these biradicaloid species have been reported,[29–31] the electronic structure of such compounds still remains unexplained due to the lack of clear-cut evidences. Recently, Zeng *et al.* reported the thermal isomerization from the biradical to quinoid states of the derivative of Chichibabin's hydrocarbon stabilized by benzannulation of the central biphenyl unit with four aromatic benzene rings.[32] They noted
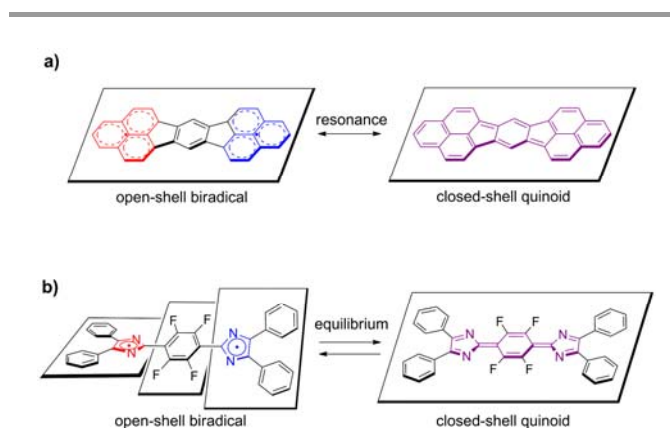
Fig. 1 a) Resonance structures of a phenalenyl framework. b) Thermal equilibrium between the biradical and quinoid forms of tF-BDPI-2Y.

the presence of an activation free energy barrier between the biradical and quinoid states. Although this is a significant observation for the thermal equilibrium in the Chichibabin's hydrocarbon derivative, the reason why the activation free energy barrier between the biradical and quinoid states exists for the flexible molecular system was not necessarily proved. This is because the molecule shows large structural change during the isomerization, which requires both large activation enthalpy ($\Delta H^{\ddagger}$) and entropy ($\Delta S^{\ddagger}$) to rotate and rearrange the molecular structure. To investigate the fundamental insight into the thermal equilibrium between the biradical and quinoid
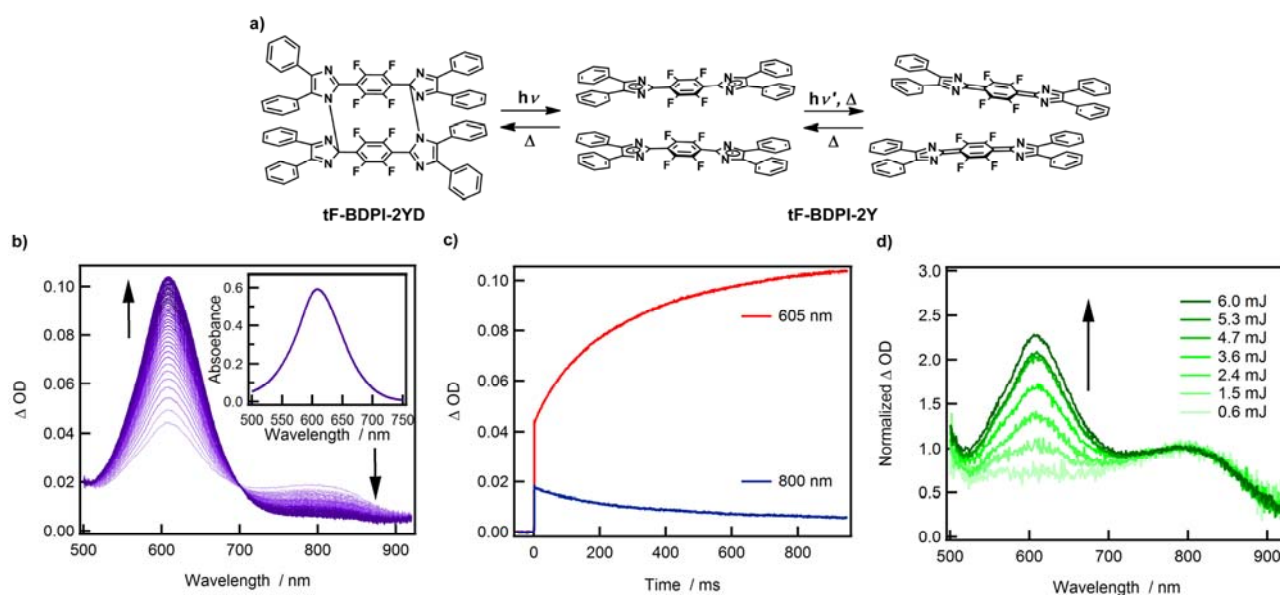
Fig. 2 a) Photochromic reaction of tF-BDPI-2YD. b) Transient absorption spectra of tF-BDPI-2YD in benzene at 298 K (2×10^{-4} M; 10 mm light path length). Each spectrum was recorded at 20 ms intervals from 2 ms after the excitation with a nanosecond laser pulse (excitation wavelength, 355 nm; pulse width, 5 ns; power, 6 mJ/pulse). The inset shows the absorption spectrum after repeating the UV light irradiation. c) Time profiles of the transient absorbances of the colored species of tF-BDPI-2YD at 605 and 800 nm in benzene at 298 K. d) The laser power dependence on the transient absorption spectra at 2 ms after the laser excitation (excitation wavelength, 355 nm; pulse width, 5 ns) to the benzene solution of tF-BDPI-2YD at 298 K (1.6×10^{-5} M; 10 mm light path length).

states, more simple molecular design is preferable to suppress large structural changes.

Our earlier studies provided the evidence for the contribution of the thermally excited open-shell state with biradical character in the closed-shell quinoid state of a BDPI-2Y derivative, tF-BDPI-2Y, where four hydrogen atoms at the central phenylene ring of BDPI-2Y are substituted with four fluorine atoms (Fig. 2a).[31,33] tF-BDPI-2Y is thermally converted to a colorless photochromic dimer (tF-BDPI-2YD) through the radical recombination reaction. The colorless benzene solution of tF-BDPI-2YD quickly turns to purple-blue upon continuous UV light irradiation and generates the quinoid species of tF-BDPI-2Y, which has an absorption maximum at 609 nm. The color gradually faded with a decrease in the absorbance in the dark. The molecular structures of tF-BDPI-2YD and tF-BDPI-2Y have been determined by X-ray crystallographic analysis.[31,33] Although the evidence for the thermal equilibrium between the open-shell biradical state and the closed-shell quinoid state of tF-BDPI-2Y was not clarified in our previous studies, this system has a potential advantage to investigate the equillibrium because the generation of the biradical species from tF-BDPI-2YD is controlled by UV light irradiation. Moreover, the simple molecular structure of tF-BDPI-2Y is suitable for investigating the thermochemical kinetics for the biradical–quinoid equilibrium because the large $\Delta H^{\ddagger}$ associated with the rotation and rearrangement of the molecular structure is suppressed. In this study, we applied the photochromic reaction of tF-BDPI-2YD to demonstrate the evidence for the thermal equilibrium between the biradical and quinoid states of tF-BDPI-2Y.

Experimental Details

Laser flash photolysis in microsecond time region

For laser flash photolysis measurements in microsecond time region with an intensified CCD (ICCD), the sample was excited with a 10 Hz Q-switch Nd:YAG laser (Continuum Surelite II; 355 nm). The excitation power and the pulse duration were 0.2 mJ/pulse and 5 ns, respectively. The halogen lamp (OSRAM HLX64623) was focused into the sample as a probe light. The transmitted light was collected by an optical fiber and detected by an ICCD-spectrometer combination (Andor Technology iStar DH320T-18U-03 and Shamrock 163). The gate duration of the ICCD is set to 50 μs and a spectrum was obtained by the average of 60 scans. The concentration of the sample was 7×10^{-5} M and the solution was continuously flowed during the experiment with a flow rate of 0.8 mL/sec to avoid the multiple excitations. The custom quartz cuvette was used for the experiment and the optical path length was 2 mm. Optical grade solvents were used for all measurements.

Laser flash photolysis in millisecond time region

The laser flash photolysis experiments were carried out with a TSP-1000 time resolved spectrophotometer (Unisoku). A 10 Hz Q-switched Nd:YAG laser (Continuum Minilite II) with the third harmonic at 355 nm (5 ns/pulse) was employed for the excitation light. The probe beam from a halogen lamp (OSRAM HLX64623) was guided with an optical fiber scope to be arranged in an orientation perpendicular to the exciting laser beam. The probe beam was monitored with a photomultiplier tube (Hamamatsu R2949) through a spectrometer (Unisoku MD200) for the time profile for the
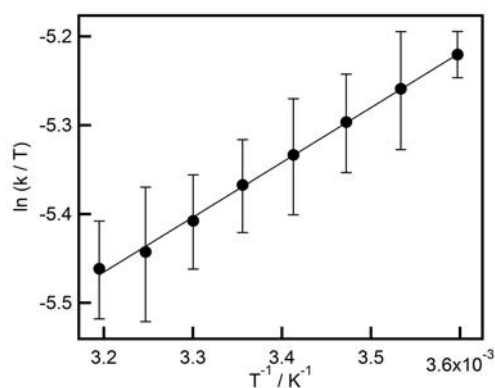
Fig. 3 Eyring plots for the thermal valence isomerization from the biradical to quinoid species in benzene. The rate constants at variable temperatures (278–313 K) are estimated as the average of at least 9 times measurements.

Fig. 4 Reaction scheme of tF-BDPI-2YD. The biradical species immediately generates from tF-BDPI-2YD via the dissociative potential upon UV light irradiation. The biradical species has three reaction pathways: i) the intermolecular thermal recombination reaction dominated by the diffusion, ii) photo-isomerization into the quinoid species through the excited state, and iii) extremely slow thermal isomerization into the quinoid species dominated by the negative $\Delta H^{\ddagger}$ and large negative $\Delta S^{\ddagger}$.

thermal isomerization and with multi-channel spectrophotometer (Unisoku MSP-1000-V1) for the transient absorption spectroscopy. Optical grade solvents were used for all measurements.

Results and Discussion tF-BDPI-2YD was prepared according to the same procedure as reported in our previous paper.[33] Nanosecond laser flash photolysis measurements were performed for the benzene solution of tF-BDPI-2YD at room temperature. Fig. 2b shows the transient absorption spectra of tF-BDPI-2YD after the 355 nm pulse excitation. Two absorption bands are observed at 609 and 800 nm after the laser irradiation. The absorption band at 800 nm gradually decreases and that at 609 nm increases with an isosbestic point, suggesting a thermal isomerization between two distinguishable states. This thermal isomerization follows the first-order kinetics and takes a few seconds to complete the reaction at room temperature (Fig. 2c and S3, ESI†). The absorption band at 609 nm is identical to that of the quinoid species as reported previously.[31] The absorption band at 800 nm can be tentatively assigned to the biradical species photochemically generated by the homolytic bond cleavage of the C–N bonds between the imidazole rings. The increment of ΔOD value at 609 nm is larger than the decrement at 800 nm, indicating that the extinction coefficient of the quinoid species is larger than that of the biradical species. When the C=C double bond of π-electron systems is twisted, the resonance integral between the adjacent p-orbitals on the carbon atoms reduces, which induces the destabilization of the HOMO energy and the stabilization of the LUMO energy.[34] Thus the twisting of the C=C double bond results in the redshift of the absorption band corresponding to the HOMO-LUMO transition. Moreover, the overlap integral decreases as well by twisting of the C=C double bond, which results in the decrease in the oscillator strength of the transition. The quinoid species of tF-BDPI-2Y has the rigid planar structure owing to the C=C double bonds between the central phenylene group and the imidazole rings. On the other hand, the biradical conformation would be more twisted in solution, since the C=C bond

character of the biradical species decreases. From this point of view, the absorption band of the biradical species shifts to the longer wavelength and the extinction coefficient of the biradical species is smaller than that of the quinoid species. Therefore, the temporal spectral changes can be explained by the thermal valence isomerization from the biradical to the quinoid species. That is, there is an activation free energy barrier between these states. Fig. S2 (ESI†) shows the transient absorption spectra in the μs time region. The transient spectra at the μs time scale are very similar with each other until 2 ms. The above described results suggest that there is a large activation free energy barrier along the isomerization reaction coordinate, and tF-BDPI-2Y has distinguishable thermally-equilibrated biradical and quinoid states. The thermal recombination reaction of tF-BDPI-2Y to form tF-BDPI-2YD is observed over a period of two days at room temperature in the dark. It is quite understandable that the dimerization reaction proceeds from only the thermally accessible biradical species.

On the other hand, the repetitive exposure of UV light pulses to the solution of tF-BDPI-2YD causes the disappearance of the 800 nm absorption band and only the absorption band at 609 nm is observed (Fig. 2b inset). As shown in Fig. 2d, the fraction of the quinoid species depends on the laser intensity. The ΔOD value at 609 nm is proportional to the amount of the quinoid species and increases with increasing the excitation laser intensity, inidicating that the biradical species also photochemically isomerizes to the quinoid species. We previously reported that the photodissociation of hexaarylbiimidazole (HABI) into the geminate radical pair occurs via the singlet excited state with a time constant of 80 fs.[35,36] By assuming the similar ultrafast bond breaking for tF-BDPI-2YD, the irradiation with a ns laser pulse would cause the photoisomerization of the radical species of tF-BDPI-2Y. To the best of our knowledge, this is the first report of the

photo-isomerization from a biradical species to a quinoid species. This result also supports the presence of the biradical and quinoid states in tF-BDPI-2Y.

The rate constants of the thermal isomerization from the biradical to quinoid species were analyzed over temperatures ranging from 278 and 313 K to determine the thermal activation parameters (Table S1, ESI†). We found that the reaction rate for the valence isomerization slightly accelerates with decreasing the temperature while those for common chemical reactions decelerate at lower temperature. The Eyring plots produce an straight line (Fig. 3), and the $\Delta H^{\ddagger}$ and $\Delta S^{\ddagger}$ values estimated from standard least-square analysis of the Eyring plots are -5.1 ± 0.1 kJ mol^{-1} and -259.4 ± 0.3 J K^{-1} mol^{-1}, respectively. The free-energy barrier $\Delta G^{\ddagger}$ (= $\Delta H^{\ddagger} - T\Delta S^{\ddagger}$) is 72.2 ± 0.2 kJ mol^{-1} at 298 K. The negative temperature dependence of the valence isomerization rate can be explained as a result of the negative $\Delta H^{\ddagger}$ (Fig. 4). In the common chemical reaction, the $\Delta H^{\ddagger}$ is usually a positive value because common chemical reactions induce bond dissociations or large conformational changes, *e.g.* rotation and inversion, between the initial state and the transition state.[37] The total enthalpy change of a reaction is determined by considering the enthalpy changes accompanied by the bond-dissociation, bond-formation, rotation and inversion. The biradical species of tF-BDPI-2Y is stabilized by making the C=C double bonds between the imidazole rings and the central phenylene ring to form the the quinoid species through the valence isomerization, although the central phenylene ring loses the aromaticity. The $\Delta H^{\ddagger}$ for the biradical–quinoid isomerization of tF-BDPI-2Y is estimated to be almost zero and rather a negative value. On the other hand, the diatomic reaction of iodine atoms has been investigated as a simple model for a radical recombination reaction and the negative activation energies for diatomic reactions have been demonstrated.[38-41] Therefore, the negative $\Delta H^{\ddagger}$ for the valence isomerization of tF-BDPI-2Y suggests that the valence isomerization is simply described as the recombination reaction of unpaired electrons as well as diatomic reactions.

Thus the large negative $\Delta S^{\ddagger}$ is found to contribute to the positive value of $\Delta G^{\ddagger}$, resulting in the extremely slow valence isomerization of tF-BDPI-2Y. Generally, an isomerization reaction with a negative $\Delta S^{\ddagger}$ indicates the conformational change from a disordered structure of the initial state to an ordered structure of the transition state. The most plausible interpretations of the large negative $\Delta S^{\ddagger}$ for the thermal isomerization of tF-BDPI-2Y is the large entropy change related to the formation of C=C double bonds. The C–C bonds between the imidazole rings and the central phenylene ring of the transition state for the valence isomerization is expected to have double-bond character compared with those of the biradical species. Consequently, the potential curve along the vibrational and rotational coordinates related to the C=C double bond of the transition state, such as the C–C stretching and the rotation between the central phenylene ring and the imidazole rings, would be steeper than those of the biradical state. Thus we came up with an idea that the difference in canonical distributions would cause the large negative $\Delta S^{\ddagger}$ between the biradical and transition states of tF-BDPI-2Y. The theoretical calculations are necesarry to gain more insight of the large negative $\Delta S^{\ddagger}$.

Conclusion

We found that the $\Delta S^{\ddagger}$ determines the electronic structure of the biradicaloid species: resonance hybrid of biradical and quinoid structures or distinguishable thermally-equilibrated biradical and quinoid states. The biradicaloid species with the rigid molecular frameworks such as phenalenyl derivatives have small entropy differences between these states. Therefore, inherently, there is no activation free energy barrier, resulting in the resonance hybrid between a biradical structure and a quinoid structure. On the other hand, we investigated a molecule with a flexible molecular framework, tF-BDPI-2Y whose biradical species is more flexible than the quinoid species due to the central single bond character, which possesses the large negative $\Delta S^{\ddagger}$, the small $\Delta H^{\ddagger}$, and the positive $\Delta G^{\ddagger}$ for the valence isomerization. Thus tF-BDPI-2Y has distinguishable thermally-equilibrated biradical and quinoid states. It is concluded that the sign and magnitude of $\Delta S^{\ddagger}$ would be an effective scale for the molecular design of biradicaloid species. The further theoretical investigation of biradicaloid species possessing flexible molecular structures will lead to a deeper understanding of our observation.

Acknowledgements

Notes and references

[a] Department of Chemistry, School of Science and Engineering, Aoyama Gakuin University, 5-10-1 Fuchinobe, Chuo-ku, Sagamihara, Kanagawa 252-5258, Japan; jiro_abe@chem.aoyama.ac.jp
[b] Itoh Optical Industrial Co.,Ltd., 3-19 Miyanari-cho, Gamagori, Aichi 443-0041, Japan
[c] Department of Chemistry, Graduate School of Science, Hiroshima University, 1-3-1 Kagamiyama, Higashi-Hiroshima, Hiroshima 739-8526, Japan
[d] CREST, Japan Science and Technology Agency, K's Gobancho, 7 Gobancho, Chiyoda-ku, Tokyo 102-0076, Japan

1   J. Kolc and J. Michl, *J. Am. Chem. Soc.*, 1973, **95**, 7391–7401.

2   C. R. Flynn and J. Michl, *J. Am. Chem. Soc.*, 1974, **96**, 3280–3288.

3   S. D. Kahn, W. J. Hehre and J. A. Pople, *J. Am. Chem. Soc.*, 1987, **109**, 1871–1873.

4   P. Piotrowiak and G. Strati, *J. Am. Chem. Soc.*, 1996, **118**, 8981–8982.

5   J. Gräfenstein, A. M. Hjerpe, E. Kraka and D. Cremer, *J. Phys. Chem. A*, 2000, **104**, 1748–1761.

6   T. Kubo, A. Shimizu, M. Sakamoto, M. Uruichi, K. Yakushi, M. Nakano, D. Shiomi, K. Sato, T. Takui, Y. Morita and K. Nakasuji, *Angew. Chem. Int. Ed.*, 2005, **44**, 6564–6568.

7   T. Kubo, Y. Goto, M. Uruichi, K. Yakushi, M. Nakano, A. Fuyuhiro, Y. Morita and K. Nakasuji, *Chem. Asian. J.*, 2007, **2**, 1370–1379.

8   A. Shimizu, T. Kubo, M. Uruichi, K. Yakushi, M. Nakano, D. Shiomi, K. Sato, T. Takui, Y. Hirao, K. Matsumoto, H. Kurata, Y. Morita and K. Nakasuji, *J. Am. Chem. Soc.*, 2010, **132**, 14421–14428.

9   M. Nakano, H. Nagao and K. Yamaguchi, *Phys. Rev. A*, 1997, **55**, 1503–1513.

10 M. Nakano, R. Kishi, T. Nitta, T. Kubo, K. Nakasuji, K. Kamada, K. Ohta, B. Champagne, E. Botek and K. Yamaguchi, *J. Phys. Chem. A*, 2005, **109**, 885–891.

11 M. Nakano, R. Kishi, N. Nakagawa, S. Ohta, H. Takahashi, S. Furukawa, K. Kamada, K. Ohta, B. Champagne, E. Botek, S. Yamada and K. Yamaguchi, *J. Phys. Chem. A*, 2006, **110**, 4238–4243.

12 K. Kamada, K. Ohta, T. Kubo, A. Shimizu, Y. Morita, K. Nakasuji, R. Kishi, S. Ohta, S. Furukawa, H. Takahashi and M. Nakano, *Angew. Chem. Int. Ed.*, 2007, **46**, 3544–3546.

13 J. Huang and M. Kertesz, *J. Am. Chem. Soc.*, 2007, **129**, 1634–1643.

14 S. Cho, J. M. Lim, S. Hiroto, P. Kim, H. Shinokubo, A. Osuka and D. Kim, *J. Am. Chem. Soc.*, 2009, **131**, 6412–6420.

15 H. Kishida, K. Hibino, A. Nakamura, D. Kato and J. Abe, *Thin Solid Films*, 2010, **519**, 1028–1030.

16 D. Bijl, H. Kainer and A. C. Rose-Innes, *J. Chem. Phys.*, 1959, **30**, 765–770.

17 S. Hiroto, K. Furukawa, H. Shinokubo and A. Osuka, *J. Am. Chem. Soc.*, 2006, **128**, 12380–12381.

18 D. Kato, K. Inoue, J. Akimitsu and J. Abe, *Chem. Lett.*, 2008, **37**, 694–695.

19 X. Zhu, H. Tsuji, K. Nakabayashi, S. Ohkoshi and E. Nakamura, *J. Am. Chem. Soc.*, 2011, **133**, 16342–16345.

20 M. Bendikov, H. M. Duong, K. Starkey, K. N. Houk, E. A. Carter and F. Wudl, *J. Am. Chem. Soc.*, 2004, **126**, 7416–7417.

21 A. Shimizu, M. Uruichi, K. Yakushi, H. Matsuzaki, H. Okamoto, M. Nakano, Y. Hirao, K. Matsumoto, H. Kurata and T. Kubo, *Angew. Chem. Int. Ed.*, 2009, **48**, 5482–5486.

22 A. Konishi, Y. Hirao, M. Nakano, A. Shimizu, E. Botek, B. Champagne, D. Shiomi, K. Sato, T. Takui, K. Matsumoto, H. Kurata and T. Kubo, *J. Am. Chem. Soc.*, 2010, **132**, 11021–11023.

23 Z. Sun, S. Lee, K. H. Park, X. Zhu, W. Zhang, B. Zheng, P. Hu, Z. Zeng, S. Das, Y. Li, C. Chi, R.-W. Li, K.-W. Huang, J. Ding, D. Kim and J. Wu, *J. Am. Chem. Soc.*, 2013, **135**, 18229–18236.

24 C. A. Hutchison, Jr., A. Kowalsky, R. C. Pastor and G. W. Wheland, *J. Chem. Phys.*, 1952, **20**, 1485–1486.

25 D. C. Reitz and S. I. Weissman, *J. Chem. Phys.*, 1960, **33**, 700–704.

26 U. Mayer, H. Baumgärtel and H. Zimmermann, *Angew. Chem.*, 1966, **78**, 303.

27 F. Popp, F. Bickelhaupt and C. Maclean, *Chem. Phys. Lett.*, 1978, **55**, 327–330.

28 L. K. Montgomery, J. C. Huffman, E. A. Jurczak and M. P. Grendze, *J. Am. Chem. Soc.*, 1986, **108**, 6004–6011.

29 A. Kikuchi, H. Ito and J. Abe, *J. Phys. Chem. B*, 2005, **109**, 19448–19453.

30 A. Rebmann, J. Zhou, P. Schuler, H. B. Stegmann and A. Rieker, *J. Chem. Research (S)*, 1996, 318–319.

31 A. Kikuchi and J. Abe, *Chem. Lett.*, 2005, **34**, 1552–1553.

32 Z. Zeng, Y. M. Sung, N. Bao, D. Tan, R. Lee, J. L. Zafra, B. S. Lee, M. Ishida, J. Ding, J. T. L. Navarrete, Y. Li, W. Zeng, D. Kim, K. Huang, R. D. Webster, J. Casado and J. Wu, *J. Am. Chem. Soc.*, 2012, **134**, 14513–14525.

33 A. Kikuchi, F. Iwahori and J. Abe, *J. Am. Chem. Soc.*, 2004, **126**, 6526–6527.

34 H. Yamashita and J. Abe, *J. Phys. Chem. A*, 2014, **118**, 1430–1438.

35 Y. Satoh, Y. Ishibashi, S. Ito, Y. Nagasawa, H. Miyasaka, H. Chosrowjan, S. Taniguchi, N. Mataga, D. Kato, A. Kikuchi and J. Abe, *Chem. Phys. Lett.*, 2007, **448**, 228–231.

36 H. Miyasaka, Y. Satoh, Y. Ishibashi, S. Ito, Y. Nagasawa, S. Taniguchi, H. Chosrowjan, N. Mataga, D. Kato, A. Kikuchi and J. Abe, *J. Am. Chem. Soc.*, 2009, **131**, 7256–7263.

37 M. Oliveberg, Y. J. Tan and A. R. Fersht, *Proc. Natl. Acad. Sci. U.S.A.*, 1995, **92**, 8926–8929.

38 M. I. Christie, R. G. W. Norrish and G. Porter, *Proc. R. Soc. Lond. A*, 1953, **216**, 152–165.

39 K. E. Russell and J. Simons, *Proc. R. Soc. Lond. A*, 1953, **217**, 271–279.

40 D. L. Bunker and N. Davidson, *J. Am. Chem. Soc.*, 1958, **80**, 5090–5096.

41 G. Porter and J. A. Smith, *Nature*, 1959, **184**, 446–447.